Suppression of super- and subradiant emission from a line of Cs atoms interacting with a resonant plane sapphire surface

M. O. Araújo and J. C. de Aquino Carvalho
Departamento de Física, Universidade Federal de Pernambuco, 50670-901, Recife, Pernambuco, Brazil

Ph. W. Courteille
Instituto de Física de São Carlos, Universidade de São Paulo, SP 13566-970 São Carlos, Brazil

A. Laliotis
Laboratoire de Physique des Lasers, UMR 7538 du CNRS,
Université Sorbonne Paris Nord, F-93430 Villetaneuse, France
(Dated: March 27, 2024)

Cooperative effects such as super- and subradiance can be observed in the fluorescence emitted by a system of N atoms in vacuum, after interaction with a laser beam. In the vicinity of a dielectric or metallic surface, Casimir-Polder effects can modify collective atomic frequency shifts and decay rates. In this work we consider a line of cesium atoms driven on their $6D_{3/2} \rightarrow 7P_{1/2}$ transition, and we show that cooperative effects, expected in free space, are suppressed when the atoms are close to a sapphire surface. This suppression is related to surface polaritons, which is demonstrated by the recovery of the cooperative effects when surface polaritons are absent.

I. INTRODUCTION

When many atoms in vacuum interact with a coherent laser beam, the resonance fluorescence emitted by them may present cooperative effects, studied extensively following the seminal work of Dicke [1]. Cooperative effects arise from quantum coherence created between the atoms if their relative distances are small, and the spontaneous emission has its decay rate enhanced. This enhancement, known as superradiance, was initially studied in the regime of many excited atoms in vapors [2], but even if a single atom is excited, a situation known as single-photon superradiance [3, 4], fast decay rates and frequency shifts can be observed.

In those cases, a system of N two-level atoms with at most one quantum of excitation is prepared from laser excitation at low intensity and far detuning [4]. The system achieves a symmetric quantum state, called timed-Dicke state, and other $N-1$ anti-symmetric states, called subradiant states [5, 6]. The emission dynamics can be obtained from the so-called coupled-dipoles model [7, 8], which treats the atoms as oscillating dipoles interacting with the eletromagnetic vacuum modes and a plane wave of incident light. Superradiance [9–12], subradiance [13, 14] and cooperative Lamb shift [11, 15] were predicted and observed experimentally in the last decades, mainly in cold ensembles of atoms but also in hot vapors [16, 17], optical lattices [18, 19] and Bose-Einstein condensates [20]. Cooperative effects were predicted and/or observed also in other observables, such as the radiation pressure force [21] and intensity correlation functions [22, 23], and in non-linear phenomena [24], spectral broadening [25] and resonance fluorescence [26]. Also, the interplay between subradiance and radiation trapping [27, 28] was investigated with cold atomic clouds, as well as the role played by finite temperature [29, 30]. Applications are, among others, ultranarrow bandwidth laser emission [31] and quantum information [32].

Vacuum fluctuations are responsible for spontaneous emission and the displacement of energy levels of an isolated atom. These fluctuations also cause the Casimir force, in which two (massive) bodies, very close to each other, tend to mutually attract due to the decrease in energy density with respect to free space. An analogous effect is observed when one of the plates is replaced by a quantum object such as an atom. This interaction between atom and surface is known as Casimir-Polder interaction [33]. When the atom is located at distances smaller than the reduced wavelength of a transition ($\lambda/2\pi$), the Casimir-Polder interaction is the near-field regime (also known as van der Waals regime) [33]. In this near-field regime, the atom-surface interaction can be viewed as an interaction between a floating atomic dipole with its own surface-induced image. This dipole-dipole interaction has a potential of the type C_3/h^3, where C_3 is the van der Waals coefficient and h is the distance between the surface and the atom. C_3 for a given state $|i\rangle$ is calculated as the sum of all allowed dipolar couplings $|j\rangle$ with frequency ω_{ij} (for emission $\omega_{ij} > 0$ and for absorption $\omega_{ij} < 0$). For an ideal conductor, we simply have $C_3 = \frac{1}{12}\sum_j |\langle i|\mu|j\rangle|^2$, where $\langle i|\mu|j\rangle$ is the dipole moment matrix element. However, for an accurate interpretation of an interaction between atoms and a dielectric surface, it is necessary to insert the permittivity properties of the dielectric through the image coefficient $r(\omega_{ij})$ at zero temperature given by [34, 35],

$$r(\omega_{ij}) = \frac{2}{\pi}\int_0^\infty S(i\xi)\frac{\omega_{ij}}{\xi^2+\omega_{ij}^2}d\xi - 2\mathrm{Re}\left[S(\omega_{ij})\right] \quad (1)$$

where the first term can be seen as a renormalization of the vacuum due to the presence of the surface and the second term resembles the interaction of a classical dipole

with its own field reflected at the surface [36]. In Eq. (1), $S(\omega) = \frac{\varepsilon(\omega)-1}{\varepsilon(\omega)+1}$ is the surface response, with $\varepsilon(\omega)$ the complex permittivity of the surface. Note that there might exist a frequency ω where $\varepsilon(\omega) = -1$ and, consequently, where $S(\omega)$ diverges. This ω is known as surface polariton frequency. When an atomic transition frequency ω_{ij} coincides with a surface polariton frequency, we say that we are in the atom-surface resonant interaction regime. These resonant effects can make the atom-surface interaction go from attractive to repulsive as well as influence the lifetime of excited states (see for example the references [37, 38]). Temperature effects may also have an impact on the atom-surface interaction [35, 39, 40] and have been observed in both, non-resonant [41] and resonant cases [42].

Theoretical work focuses on the calculation of corrections to the energies and decay rates from second-order perturbation theory in the interaction Hamiltonian between atom and surface for a single atom [36]. Another approach consists in determining the Green function in terms of the Fresnel coefficients from the interaction between atom and the surface-modified electric field [43] for one and two atoms embedded in a multilayer dielectric [43, 44]. Interplay between cooperative effects and Casimir-Polder interactions was also predicted theoretically. For two Rb atoms, cooperative decay rates and shifts were predicted to be modified due to Fano resonances, when the atoms are near a nanosphere [45]. For $N > 2$ atoms near a surface, theoretical work predicted changes in superradiance [46] and of the Casimir-Polder force in the regime of many excitations [46, 47]. An approach based on the calculation of frequency shifts and decay rates from the Green matrix was done for a line of two to twenty atoms interacting with an Ag surface [48]. However, work on atoms interacting with surfaces are still scarce, specially when atoms and surface are in resonance.

The control of cooperative effects, in particular, subradiance, is interesting for applications in quantum information, for example, fast readout [49] and the generation of entangled states [50]. In this work, we study the possibility of coupling super- and subradiant modes with surface-induced resonances. Contrary to refs. [46, 47], which observed an enhancement of the Casimir-Polder forces for $N \gg 1$ excited atoms close to a surface, here we study the linear-optics regime by means of a line of N Cs atoms interacting with a resonant sapphire surface, in the single-excitation limit. Sapphire has a resonance at the wavelength $\lambda_s = 12$ μm, whereas Cs exhibits a decay transition $6D_{3/2} \rightarrow 7P_{1/2}$ with $\lambda = 12.15$ μm. This gives $\varepsilon \approx -1$ and surface polaritons appear, in addition to the modified vacuum evanescent modes. By evaluating the emitted fluorescence from the coupled-dipoles model after the system has reached a steady state, we show that super- and subradiance are suppressed due to the surface polaritons, and the fluorescence of the whole system decays as if a single atom was placed close to the surface. In the absence of surface polaritons, i.e., for interaction of Cs with glass or a metallic surface, i.e., $|\lambda_s - \lambda| \gg \lambda$, cooperative effects are not suppressed, although modified, because the evanescent modes created by the surface are still present.

This paper is organized as follows. In section II, we review the approach for cooperative effects and surface interactions for N atoms (subsections II A and II B) and then present a modified coupled-dipoles model taking into account surface effects (II C), in order to evaluate the decay dynamics of the atoms. In section III we present our simulation methods, and the main results are presented in section IV. We make our concluding remarks in section V.

II. THEORETICAL MODEL

A. Atoms in free space and close to a plane surface

The formalism used here is the same as presented in [43, 44, 48], which considers dipoles in vacuum close to a plane surface, in such a way that the vacuum and the surface form a two-layer medium. We consider a line of N identical two-level atoms with resonance frequency ω_0, transition wavelength λ and same dipole orientations $\hat{\mathbf{d}}$ (Fig. 1) [62]. The atomic levels of the atom j are denoted by $|g_j\rangle$ ($|e_j\rangle$) for the ground (excited) state, with $j = 1, ..., N$. All atoms are fixed at positions $\mathbf{r}_a = (x_a, y_a, z_a)$ and placed at a distance h from the surface of a plane dielectric occupying the half space $z \leq 0$. The other half space $z \geq 0$ is vacuum. A monochromatic plane wave of frequency ω and detuning $\Delta = \omega - \omega_0$ is incident along the z axis and illuminates all atoms.

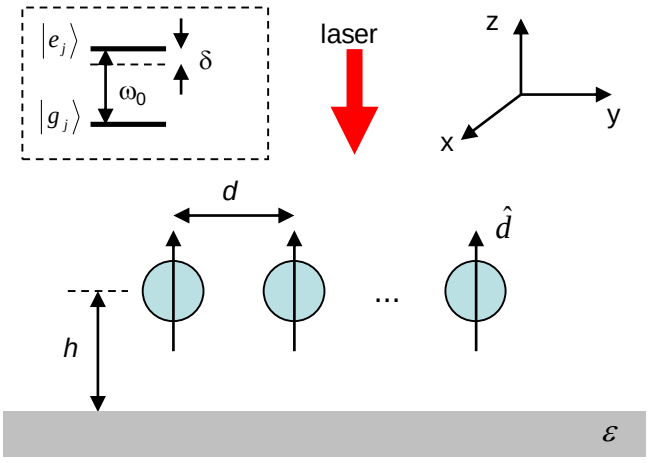

FIG. 1. Scheme of the physical system. A line of N identical two-level atoms is placed at identical distances h from a planar surface lying on the semi-infinite $z \leq 0$ plane. The atoms are distributed with equal distances d along the y-axis and have their dipoles orientated in the direction $\hat{\mathbf{d}} = \hat{\mathbf{z}}$, i.e., perpendicularly to the surface. A laser beam of frequency ω pointing into the $-\hat{\mathbf{z}}$ direction drives the atoms. Inset: Scheme of the two atomic levels.

The Heisenberg-Liouville equation for the Pauli spin-down operator acting on atom a reads

$$\dot{\hat{\sigma}}_a^- = -\tfrac{i}{\hbar}[\hat{\sigma}_a^-, \hat{H}] + \mathfrak{L}^\dagger[\hat{\sigma}_a^-] \tag{2}$$

where $\hat{\sigma}_a^- = |g_a\rangle\langle e_a|$ is the atomic operator. The Hamiltonian and dissipation terms are

$$\begin{aligned}\hat{H} &= -\frac{\hbar\Delta}{2}\sum_b \hat{\sigma}_b^z + \tfrac{\hbar}{2}\sum_b [\Omega(\mathbf{r}_b)\hat{\sigma}_b^+ + h.c.] - \\ &- \hbar\sum_{a,b} V_{ab}\hat{\sigma}_a^+\hat{\sigma}_b^- \end{aligned} \tag{3}$$

$$\mathfrak{L}^\dagger[\hat{A}] = \tfrac{1}{2}\sum_{a,b}\Gamma_{ab}\left(2\hat{\sigma}_a^+\hat{A}\hat{\sigma}_b^- - \hat{\sigma}_a^+\hat{\sigma}_b^-\hat{A} - \hat{A}\hat{\sigma}_a^+\hat{\sigma}_b^-\right) \tag{4}$$

where $\hat{\sigma}_a^z \equiv \hat{\sigma}_a^+\hat{\sigma}_a^- - \hat{\sigma}_a^-\hat{\sigma}_a^+$ and $\Omega(\mathbf{r})$ denotes the Rabi frequency generated by a classical incident laser beam at position $\mathbf{r}$. Collective shifts and decay rates are given by

$$V_{ab} = \lambda\Gamma\hat{\mathbf{d}}^* \mathrm{Re}\; G(\mathbf{r}_a, \mathbf{r}_b, \omega_0)\hat{\mathbf{d}} \tag{5a}$$

$$\Gamma_{ab} = 2\lambda\Gamma\hat{\mathbf{d}}^* \mathrm{Im}\; G(\mathbf{r}_a, \mathbf{r}_b, \omega_0)\hat{\mathbf{d}} \tag{5b}$$

In Eqs. (5), G is the Green tensor describing the interaction between two atoms a and b, and $\Gamma = \omega_0^3 d_{\mathrm{eg}}^2/(3\pi c^3\varepsilon_0\hbar)$ is the free-space single atom decay rate and d_{eg} is the matrix dipole element between the states $|g\rangle$ and $|e\rangle$ As in [48], we assume all dipoles to have the same orientation $\hat{\mathbf{d}}$. With this, Eq. (2) becomes

$$\begin{aligned}\dot{\hat{\sigma}}_a^- &= i\Delta\hat{\sigma}_a^- + \tfrac{i}{2}\Omega(\mathbf{r}_a)\hat{\sigma}_a^z - i\delta\hat{\sigma}_a^z\hat{\sigma}_a^- + \tfrac{\Gamma_{tot}}{2}\hat{\sigma}_a^z\hat{\sigma}_a^- \\ &- i\sum_{b\neq a}^N V_{ab}\hat{\sigma}_a^z\hat{\sigma}_b^- + \sum_{b\neq a}^N \tfrac{\Gamma_{ab}}{2}\hat{\sigma}_a^z\hat{\sigma}_b^- \end{aligned} \tag{6}$$

where $\delta \equiv V_{aa}$ and $\Gamma_{tot} \equiv \Gamma_{aa}$. This equation will be the starting point used in Sec. II C for the derivation of the coupled dipoles model, which is the basis for our numerical simulations.

Eq. (5) has been derived for free space. The presence of a surface can now be accounted for by simply adding to the free space Green function a scattering Green function

$$G = G^0 + G^{\mathrm{R}} \tag{7}$$

where G^0 is the Green tensor in free space and G^{R} is the scattering term taking into account the surface. This decomposition allows us to write

$$V_{ab} = V_{ab}^0 + V_{ab}^{\mathrm{R}} \tag{8a}$$

$$\Gamma_{ab} = \Gamma_{ab}^0 + \Gamma_{ab}^{\mathrm{R}} \tag{8b}$$

because of Eqs. (5).

B. Green tensor for free space and surface

The Green tensor for free space, G^0, is given in [48, 51]. Eqs. (5) with $G = G^0$ then lead to [48]

$$\begin{aligned}V_{ab}^0 &= \frac{\Gamma}{2}\Big[(1-(\hat{\mathbf{d}}\cdot\hat{\mathbf{r}}_{ab})^2)\frac{\cos\kappa_{ab}}{\kappa_{ab}} - \\ &- (1-3(\hat{\mathbf{d}}\cdot\hat{\mathbf{r}}_{ab})^2)\left(\frac{\sin\kappa_{ab}}{\kappa_{ab}^2} + \frac{\cos\kappa_{ab}}{\kappa_{ab}^3}\right)\Big] \end{aligned} \tag{9a}$$

$$\begin{aligned}\Gamma_{ab}^0 &= \Gamma\Big[(1-(\hat{\mathbf{d}}\cdot\hat{\mathbf{r}}_{ab})^2)\frac{\sin\kappa_{ab}}{\kappa_{ab}} + \\ &+ (1-3(\hat{\mathbf{d}}\cdot\hat{\mathbf{r}}_{ab})^2)\left(\frac{\cos\kappa_{ab}}{\kappa_{ab}^2} - \frac{\sin\kappa_{ab}}{\kappa_{ab}^3}\right)\Big] \end{aligned} \tag{9b}$$

where $\kappa_{ab} = kr_{ab}$, $r_{ab} = |\mathbf{r}_{ab}| = |\mathbf{r}_a - \mathbf{r}_b|$ is the relative distance between the atoms a and b and $\hat{\mathbf{r}}_{ab}$ is the unit vector along the direction of $\mathbf{r}_{ab}$. As pointed out by [48], the expressions (9) yield the frequency shifts and decay rates of the excited energy levels obtained in previous work [52–54]. They lead to cooperative effects as, e.g., superradiance [10, 11], subradiance [14] and cooperative Lamb shift [11]. For $a = b$, we have $V_{aa}^0 = 0$ and $\Gamma_{aa} = \Gamma$.

The Green tensor G^{R} for a surface is given in refs. [44, 48] for atoms in a multilayer dielectric, and takes into account the reflection of vacuum modes and evanescent modes created by the surface. The present case of a vacuum-dielectric interface can be seen as a two-layer dielectric, so the equations of ref. [48] simplify and read

$$G^{\mathrm{R}}(\mathbf{r}_a, \mathbf{r}_b, \omega_0) = \frac{i}{4\pi}\int_0^\infty dk_\rho \frac{k_\rho}{k_z}\left(G^{\mathrm{s}} - \frac{k_z^2}{k^2}G^{\mathrm{p}}\right) \tag{10}$$

where G^{s} and G^{p} are given by

$$G^{\mathrm{s}} = \frac{r^{\mathrm{s}}e^{2ik_z h}}{2}\begin{pmatrix} J_0 - J_2 & 0 & 0 \\ 0 & J_0 + J_2 & 0 \\ 0 & 0 & 0 \end{pmatrix} \tag{11a}$$

$$G^{\mathrm{p}} = \frac{r^{\mathrm{p}}e^{2ik_z h}}{2}\begin{pmatrix} J_0 + J_2 & 0 & 0 \\ 0 & J_0 + J_2 & \frac{2ik_\rho}{k_z}J_1\sin\phi \\ 0 & -\frac{2ik_\rho}{k_z}J_1\sin\phi & -\frac{2k_\rho^2}{k_z^2}J_0 \end{pmatrix} \tag{11b}$$

In Eqs. (11a) and (11b), $k = 2\pi/\lambda = \omega_0/c$, $k_z = \sqrt{k^2 - k_\rho^2}$ [with $\mathrm{Re}(k_z) > 0$, $\mathrm{Im}(k_z) > 0$ [43]], $J_n \equiv J_n(k_\rho|y_{ab}|)$ is the Bessel function of order n, and $\sin\phi = y_{ab}/|y_{ab}|$, which gives $\sin\phi = +1$ ($\sin\phi = -1$) for $a < b$ ($a > b$). The quantities r^q with $q = \{\mathrm{s}, \mathrm{p}\}$, are the Fresnel coefficients and are given by

$$r^s = \frac{k_z - k_{IIz}}{k_z + k_{IIz}} \tag{12a}$$

$$r^p = \frac{\epsilon(\omega)k_z - k_{IIz}}{\epsilon(\omega)k_z + k_{IIz}} \tag{12b}$$

with $k_{IIz} = \sqrt{\epsilon(\omega)k^2 - k_\rho^2}$, [$\mathrm{Re}(k_{IIz}) > 0$ and $\mathrm{Im}(k_{IIz}) > 0$].

The surface shifts $V^{\rm R}_{ab}$ and decay rates $\Gamma^{\rm R}_{ab}$ are given by Eqs. (5) with $G = G^{\rm R}$. For $a = b$, we have the Casimir-Polder shift $\delta \equiv V^{\rm R}_{aa}$ and the surface-induced decay rate $\Gamma_z \equiv \Gamma^{\rm R}_{aa}$ in a such way that the total shift and decay rate are $V_{aa} = \delta$ and $\Gamma_{aa} = \Gamma + \Gamma_z$ (Eqs. 8 with $a = b$). As pointed out by [48], the total V_{ab} and Γ_{ab} contain the cooperative effects in the sense that diagonal terms ($a = b$) contain the shifts and decay rates for a single atom modified by the surface, whereas the off-diagonal terms ($a \neq b$) measure the strength of the cooperative effects due to the coupling between atoms and surface.

For a single atom ($N = 1$) and a surface, we have $V^{\rm R}_{a\neq b} = \Gamma^{\rm R}_{a\neq b} = 0$, and then we have $V_{aa} = \delta$ and $\Gamma_{aa} = \Gamma + \Gamma_z$, due to the interaction with the surface. Also, it can be shown [44] that for $kh \ll 1$, the matrix terms of $G^{\rm R}$ become proportional to

$$G^{\rm R}_{ij}(\omega_0) \propto \frac{S(\omega_0)}{h^3} \tag{13}$$

for $i, j = \{x, y, z\}$, where $S(\omega) = \frac{\varepsilon(\omega)-1}{\varepsilon(\omega)+1}$ and $\varepsilon(\omega)$ is the complex electric permittivity of the surface. Eq. (13) is in agreement with Eq. (1) obtained in [36]. Note that if $\varepsilon \approx -1$ for a certain atomic transition frequency ω, a condition known as surface polariton, S diverges, and consequently $G^{\rm R}_{ij}(\omega_0)$. This resonant enhancement effect was used in hot vapors to turn an atom-surface interaction from attractive to repulsive [37] or cause the atomic emission to be absorbed by the surface [38]. As we will see in the next subsection, the fluorescence emitted by the system depends on all these terms, and the effect of this enhancement for weak excitations is to modify the decay dynamics and to extinguish cooperative effects.

C. Decay dynamics with surface

Now, we assume low atomic excitation, $\langle\hat{\sigma}^z_a\rangle \simeq -1$ (low-energy Dicke state), that is, most atoms are in the ground state. Then, we may neglect correlations ($\langle\hat{\sigma}^z_a\hat{\sigma}^-_a\rangle = \langle\hat{\sigma}^z_a\rangle\langle\hat{\sigma}^-_a\rangle$) and find from Eq. (6), with $\beta_a \equiv \langle\hat{\sigma}^-_a\rangle$,

$$\dot{\beta}_a \simeq \left(\imath\Delta_{\rm tot} - \tfrac{\Gamma_{\rm tot}}{2}\right)\beta_a - \tfrac{\imath}{2}\Omega(\mathbf{r}_a) + \sum_{b\neq a}^{N}\left(\imath V_{ab} - \tfrac{\Gamma_{ab}}{2}\right)\beta_b \tag{14}$$

where $\Delta_{\rm tot} = \Delta + \delta$ and $\Gamma_{\rm tot} = \Gamma + \Gamma_z$. In the absence of a surface, i.e., $G = G^0$, the dynamics of the N atoms interacting with vacuum and a light field was discussed extensively [53]. Driving is weak for large detunings Δ and small Rabi frequencies Ω, and under these conditions the system admits two states: the ground state $|G\rangle = |g_1...g_N\rangle$ (i.e., all N atoms are in the state $|g_j\rangle$) and N single-excitation states $|j\rangle = |g_1...e_j...g_N\rangle$ (i.e., the atom j is in the state $|e_j\rangle$ and the other $N-1$ atoms are in the state $|g_j\rangle$).

Assuming that driven by a laser field the system reached a steady-state and then the laser is turned off, i.e., $\Omega = 0$, the total fluorescence emitted by the atoms can be evaluated from [55]

$$P(t) \propto -\frac{d}{dt}\sum_{j=1}^{N}|\beta_j(t)|^2 \tag{15}$$

Signatures of cooperative effects in the fluorescence were predicted theoretically [53] and observed experimentally [10, 11, 14] in the last decade for atoms distributed in free space.

For a single atom in free space Eqs. (14) and (15) reduce to the standard fluorescence with natural exponential decay rate Γ. For a single atom near a surface Eqs. (14) and (15) reproduce the decay dynamics with surface effects. Finally, for N atoms near a surface, both surface and cooperative effects are present, and we show in the next section, that the cooperative effects are suppressed due to the surface modes when the surface is in resonance with the atomic transition, i.e., when $\varepsilon = -1$. For $\varepsilon \neq -1$, cooperative effects are slightly modified.

III. SIMULATION METHODS

A. Casimir-Polder shift for Cs atom and sapphire

Our simulation method is similar to the one described in [55]. As in [48], we simulate the simplest case of a line of N atoms distributed along the y-axis, equally spaced by a distance d, located at the same distance h from a planar surface (see Fig. 1), and having same dipole orientations $\hat{\mathbf{d}}$. That is, $x_a = 0$ and $z_a = h$ for all atoms. The incoming laser comes from the direction $-\hat{\mathbf{z}}$, i.e., it illuminates all atoms equally. Then, for a given dipole orientation $\hat{\mathbf{d}}$, we evaluate V^0_{ab} and Γ^0_{ab} from Eqs. (9). We also compute the matrix terms of $G^{\rm R}$ from Eqs. (10-11) and use them to evaluate $V^{\rm R}_{ab}$ and $\Gamma^{\rm R}_{ab}$ from Eqs. (5). Finally, we solve numerically the Eqs. (14) governing the evolutions of the $\beta_a(t)$ for a given Δ, and compute the total fluorescence $P(t)$ from Eq. (15). The fluorescence is normalized by its maximum value $P(0)$, which occurs at $t = 0$ when steady state is reached and the incident driving field is turned off.

For atoms in free space, there is no shift in the excited state, so the frequency detuning of the laser Δ is taken with respect to the excited state energy. However, for atoms in the presence of a surface, as the excited level will be shifted by δ, the laser frequency is set in a such way as to maintain the detuning from the shifted level, $\Delta_{\rm tot} = \Delta + \delta$.

We are interested in simulating Cs atoms close to a sapphire surface. Cesium has the transition decay $6D_{3/2} \to 7P_{1/2}$ with wavelength $\lambda = 12.15\,\mu$m (see Fig. 2a), while sapphire has a resonance at approximately $\lambda_{\rm s} \sim 12\,\mu$m [34], for which Re $\varepsilon \approx -1$ (Figs. 2b-c), that is, we have

a resonant atom-surface interaction. The Cesium transition has a natural decay rate of $\Gamma = 2\pi \times 14.32\,\mathrm{kHz}$ [56], although the level $6D_{3/2}$ has other decay channels, so that its total decay rate is in the range of 2.7 MHz [57]. In our model, we consider $|g\rangle \equiv |7P_{1/2}\rangle$ and $|e\rangle \equiv |6D_{3/2}\rangle$ as ground and excited states, respectively, and the atom is initially in the state $|e\rangle$, which can be prepared, e.g., by two-photon excitation from $|6S_{1/2}\rangle$ (see Fig. 2a).

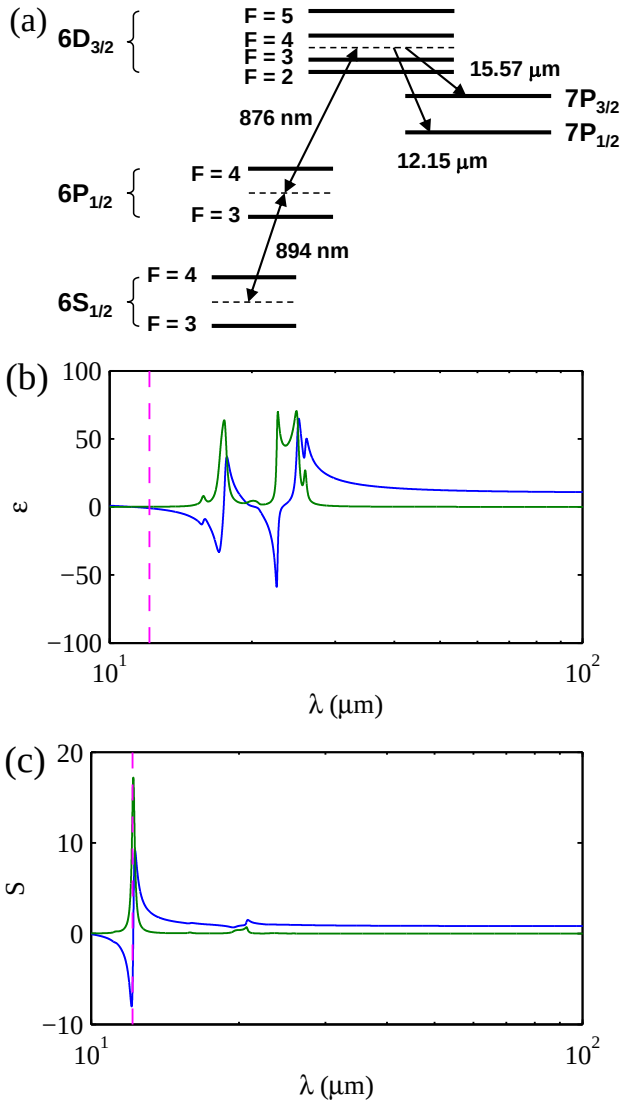

FIG. 2. (a) Schematic of Cs levels. Real (blue) and imaginary (green) parts of (b) the relative dielectric constant ε and (c) $S = (\varepsilon - 1)/(\varepsilon + 1)$ for sapphire. The dashed magenta lines indicate the value $\lambda = 12.15\,\mu\mathrm{m}$, for which $\varepsilon = -0.95 \approx -1$ and $S = \infty$.

The frequencies of the Casimir-Polder shift given in [36] hold for both ground and excited states. It can be shown that for a single atom at a distance h from a surface, we have

$$\delta = -\frac{C_3}{h^3} \tag{16}$$

TABLE I. Values of the parameters used for the simulation of a single Cs atom interacting via its transition $6D_{3/2} \rightarrow 7P_{1/2}$ with a sapphire surface. The quantities δ and Γ_z were evaluated with Eqs. (5) for $a = b$ and $G = G^{\mathrm{R}}$ (see text).

h (μm)	kh	δ/Γ	$(\Gamma + \Gamma_z)/\Gamma$
0.100	0.05	5660	29235
0.500	0.25	63	176
1	0.5	9	14
2	1	1	1.074
3	1.5	0.24	0.61
4	2	0.009	0.73
5	2.5	-0.06	0.9
10	5	0.005	0.98

where $C_3 = 13.53\,\mathrm{kHz.\mu m^3}$ ($C_3 = -100\,\mathrm{kHz.\mu m^3}$) for the $7P_{1/2}$ (excited) level [37, 42]. Γ_z has a similar dependence.

In section IV, we will consider the dipole orientation $\hat{\mathbf{d}}$ perpendicular to the surface for all atoms, i.e., $\hat{\mathbf{d}} = \hat{\mathbf{z}}$. For Cs and a sapphire surface, we checked that the direction of $\hat{\mathbf{d}}$ does not alter significantly the results. We also checked that our simulations give $\delta = -(113.39\,\mathrm{kHz.\mu m^3})/h^3$ for a single atom and sapphire, in agreement with Eq. (16) where the global shift is $|C_{3tot}| = 113.53\,\mathrm{kHz.\mu m^3}$. For interaction with metallic surfaces (ideal conductor; $\varepsilon = -\infty$), it is known that a single atom, whose dipole moment is oriented perpendicularly to the surface, interacts stronger as compared to an atom placed parallel to the surface [45, 58]. For very low distances kh from the surface (typically $h \sim 10\,\mathrm{nm}$), we have $\Gamma_z \approx 0$ ($\Gamma_z \approx 2\Gamma$) for $\hat{\mathbf{d}} \parallel \hat{\mathbf{z}}$ ($\hat{\mathbf{d}} \perp \hat{\mathbf{z}}$). We checked that our simulations reproduce this effect.

Table I shows some values of h and the corresponding values of kh, shifts, and decay rates used in our simulations, for Cs and sapphire.

IV. RESULTS AND DISCUSSION

In what follows, we consider a line of $N = 5$ Cs atoms interacting with a sapphire surface. As already mentioned, the atoms are aligned perpendicularly to the surface, i.e., $\hat{\mathbf{d}} = \hat{\mathbf{z}}$. We checked that simulations with $N = 20$, 50 and 100 atoms give the same results.

A. Suppression of the cooperative effects due to surface interactions

The main results of this paper are shown in Fig. 3, for far detuned excitation. $P(t)$ is plotted for three values of kd, for atoms far from each other (solid red and green curves) and close to each other (solid blue curves). The three panels (a), (b), and (c) correspond to atom-surface distances of $kh = 0.25$, $kh = 0.5$, and $kh = 2.5$, respectively. The fluorescence of a single atom is plotted for

comparison (black curves), as well as for atoms in free space, plotted as dashed lines. In Fig. 3a, for atoms in free space (dashed lines), no cooperative effects are seen for $kd = 3$ and $kd = 10$, because the many-atom decay is close to the single atom decay (black dashed curve). However, when the atoms are close to each other ($kd = 1$), we see that $P(t)$ presents cooperative effects: superradiance (fast decay; $\Gamma t < 4$) and subradiance (slow decay; $\Gamma t > 4$). It is worth mentioning that ref. [48] considers $kd = 0.5$ for a line of $N = 20$ atoms, where $\lambda = 2.5\,\mu$m for Sr atoms. Long-lived cooperative states were observed in free-space in this configuration [59].

The impact of the surface consists in accelerating the decay, as seen in the inset of Fig. 3a (solid lines) as almost-vertical curves, for atoms very close to the surface ($kh = 0.25$ or $h \approx 500\,$nm). The data for a single atom and for $N = 5$ for $kd = 1, 3, 10$ almost collapse into a single curve. For a single atom, we have a high value of the surface decay rate, which is equal to $\Gamma_z = 175\Gamma$ (see Table I). In [37], for a hot vapor, it was observed that the atom loses its excitation to the surface modes. For $N > 1$ atoms, we also have a fluorescence decay with a rate equal to the single-atom one. This means that subradiance, the slow decay, is completely suppressed and the predominating decay is a very enhanced superradiance, the fast decay, due to the Casimir-Polder interactions and induced by the coupling of the surface modes with the atoms.

Figures 3b and 3c show the dependence of $P(t)$ on the distance kh between the atoms and the surface. The free space data is displayed again for comparison. If the line of atoms is moved away from the surface (Fig. 3b with $kh = 0.5$), the surface interactions become weaker, and the decay slows down. For atoms very far from the surface (Fig. 3c with $kh = 2.5$), the surface effects disappear completely. In this case, we recover the original decays (solid and dashed curves coincide), and cooperative effects reappear.

We checked that similar results are obtained for atoms at resonance (i.e., $\Delta = 0$), and when the polarization of the incoming laser field is aligned with the atoms (i.e., $\hat{\mathbf{d}} = \hat{\mathbf{y}}$). In free space, subradiance at resonance has its weight increased, as observed in [55, 60], due to a larger occupation of the subradiant modes in steady state before switching off the incident driving [60]. The same occurs for laser excitation parallel to the atom line, because in this geometry the optical depth b_0 of the system is larger, and cooperative decay rates depend on b_0 [10, 11, 14]. However, similar to the far-detuned case displayed in Fig. 3, cooperative effects for $\Delta = 0$ and parallel excitation are completely suppressed due to the atom-surface interactions at small kh.

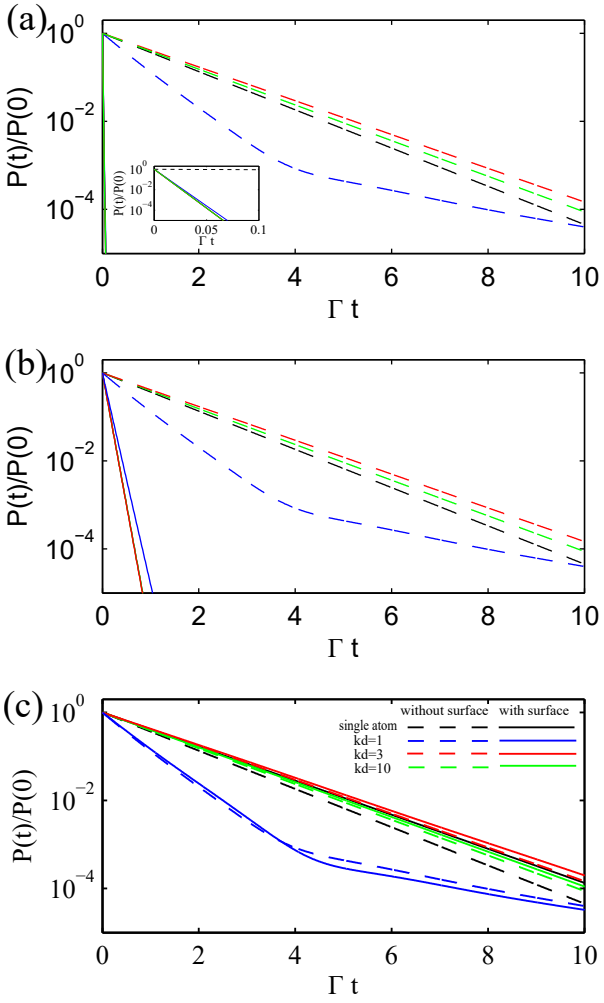

FIG. 3. Total fluorescence as a function of time for $\Delta = 10\Gamma$ and (a) $kh = 0.25$ ($h \approx 500\,$nm), (b) $kh = 0.5$ ($h \approx 1\mu$m), and (c) $kh = 2.5$ ($h \approx 5\,\mu$m). Dashed (full) lines are for atoms without (with) sapphire surface, for: $N_{\rm at} = 1$ (black), $(N_{\rm at}, kd) = (5, 10)$ (green), $(5, 3)$ (red), and $(5, 1)$ (blue). Inset: zoom on panel (a).

B. Impact of the surface resonance in the atom coupling

The Casimir-Polder effects discussed in the previous subsections are dominated by the fact that the surface is resonant with the atomic transition, i.e., $\lambda_{\rm s} \approx \lambda$ ($\varepsilon = -1$). Surfaces such as glass and metal present resonances far from the atomic transitions currently used in experiments. As an example, an Ag surface presents a resonance around 3.64 eV [48], whereas earth and earth alkali atoms have their main transitions below this value, e.g., 0.5 eV for the Sr transition $^3P_0 \rightarrow {}^3D_1$, 1.6 eV for the Rb D_2 line, 2.1 eV for the Na D_2 line, or 2.7 eV for the Sr transition $^1S_0 \rightarrow {}^1P_1$.

In order to illustrate the impact of the surface resonance, Fig. 4 displays the fluorescence $P(t)$ emitted by the atoms interacting with sapphire for four differ-

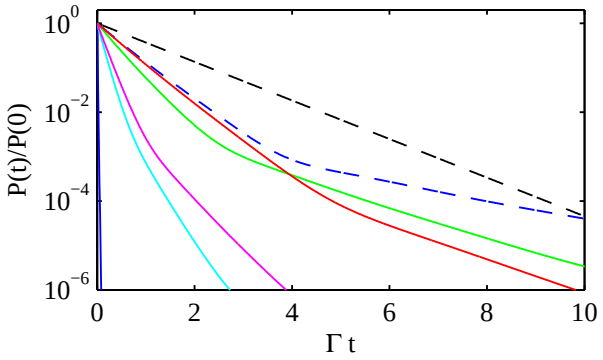

FIG. 4. Emitted fluorescence $P(t)$ for $N = 5$ atoms, $kd = 1$ and $\Delta = 10\Gamma$, interacting with surface (full lines) for the following atomic wavelengths: $\lambda = 8.15\,\mu$m (green), $10.15\,\mu$m (red), $12.15\,\mu$m (blue), $14.15\,\mu$m (cyan) and $16.15\,\mu$m (magenta). These λ give, respectively, the sapphire dielectric constants $\varepsilon = 1.8 + 0.015i$, $\varepsilon = 0.78 + 0.040i$, $\varepsilon = -0.95 + 0.11i$, $\varepsilon = -4.6 + 0.43i$ and $\varepsilon = -12 + 4.0i$. Dashed lines: decay in free space for $N = 1$ (dashed black) and $N = 5$ (dashed blue).

ent atomic wavelengths λ, below and above the resonant wavelength, $\lambda_s = 12.15\,\mu$m (we have evaluated the value of ε for sapphire for each λ). Data without surface is displayed for comparison. When the surface is not resonant with the transition wavelength, $\varepsilon \neq -1$, and this retrieves some cooperative modes, meaning that the atom-surface coupling is not strong any more. Some remaining surface effects are due to evanescent surface modes. However, for $\varepsilon = -1$, the cooperative decay is extinguished. We checked that similar results are obtained when fixing $\lambda_s = 12.15\,\mu$m but using values of ε for glass (which presents no resonance around $12\,\mu$m), an ideal metallic surface (where $\varepsilon = -\infty$) and an Ag surface.

V. CONCLUSION

In summary, we have studied the fluorescence emitted by a line of Cs atoms close to a sapphire surface in the presence of surface polaritons, i.e., when the surface is resonant with an atomic transition. We showed that the surface suppresses all cooperative modes, like super- and subradiance, which are present when the atoms are placed in free space. In the presence of sapphire, fluorescence decays as if there was a single atom near the surface. Also, when surface polaritons are absent, i.e., out of resonant coupling with the surface, the cooperative effects are not suppressed, although they are slightly modified due to the interaction with evanescent vacuum modes that are still present.

Throughout this work, we assumed total emitted fluorescence in our calculations, thanks to the non-directional character of subradiance [13]. On the other hand, the superradiant decay rate depends on direction [10], although it can be observed in all directions. Realistic geometries like a sphere would introduce different frequency surface shifts for each atom, but we expect no qualitative changes.

The control of cooperative effects, in particular subradiance, is relevant for applications in quantum information [50] and metrology [61]. An interesting example is the superradiant laser, where the collective coupling of an atomic sample to a dissipative mode, here an optical cavity operated in the 'bad cavity' limit, leads to global synchronization of the atomic dipoles [31]. The interaction with surfaces has been suggested as a possible handle for this control. It is, therefore, important to understand the impact of surfaces on collective dynamics in various circumstances. This work shows that the vicinity of polariton resonances can have a devastating effect on cooperativity. Although performed in the weak excitation limit, we believe that our results will contribute to the understanding of cooperative atom-surface coupling in the presence of many excitations.

ACKNOWLEDGEMENTS

M.O.A. and J.C. de A.C. thank UFPE for some financial support. Ph.W.C. received support from FAPESP (grant no. 2022/00209-6), from CAPES-COFECUB (Ph879-17/CAPES 88887.130197/2017-01), and from CNPq-SFSN (grant. 402660/2019-6).

[1] R. H. Dicke, Physical Review **93**, 99 (1954).
[2] M. Gross and S. Haroche, Physics Reports **93**, 301 (1982).
[3] M. O. Scully, E. S. Fry, C. H. R. Ooi, and K. Wódkiewicz, Physical Review Letters **96**, 010501 (2006).
[4] Ph. W. Courteille, S. Bux, E. Lucioni, K. Lauber, T. Bienaimé, R. Kaiser, and N. Piovella, The European Physical Journal D **58**, 69 (2010).
[5] M. O. Scully, Laser Physics **17**, 635 (2007).
[6] T. Bienaimé, *Effets coopératifs dans les nuages d'atomes froids*, Ph.D. thesis, Université Nice Sophia Antipolis (2011).
[7] A. A. Svidzinsky, J.-T. Chang, and M. O. Scully, Phys. Rev. A **81**, 053821 (2010).
[8] T. Bienaimé, M. Petruzzo, D. Bigerni, N. Piovella, and R. Kaiser, Journal of Modern Optics **58**, 1942 (2011),
[9] A. A. Svidzinsky, J.-T. Chang, and M. O. Scully, Phys. Rev. Lett. **100**, 160504 (2008).
[10] M. O. Araújo, I. Krešić, R. Kaiser, and W. Guerin, Physical Review Letters **117**, 073002 (2016).
[11] S. J. Roof, K. J. Kemp, M. D. Havey, and I. M. Sokolov, Physical Review Letters **117**, 073003 (2016).
[12] A. S. Kuraptsev, I. M. Sokolov, and M. D. Havey, Physical Review A **96**, 023830 (2017).

[13] T. Bienaimé, N. Piovella, and R. Kaiser, Physical Review Letters **108**, 123602 (2012).
[14] W. Guerin, M. O. Araújo, and R. Kaiser, Physical Review Letters **116**, 083601 (2016).
[15] M. O. Scully, Physical Review Letters **102**, 143601 (2009).
[16] J. Keaveney, A. Sargsyan, U. Krohn, I. G. Hughes, D. Sarkisyan, and C. S. Adams, Phys. Rev. Lett. **108**, 173601 (2012).
[17] T. Peyrot, Y. R. P. Sortais, A. Browaeys, A. Sargsyan, D. Sarkisyan, J. Keaveney, I. G. Hughes, and C. S. Adams, Phys. Rev. Lett. **120**, 243401 (2018).
[18] B. Olmos and I. Lesanovsky, Phys. Rev. A **82**, 063404 (2010).
[19] A. Schilke, C. Zimmermann, Ph. W. Courteille, and W. Guerin, Phys. Rev. Lett. **106**, 223903 (2011).
[20] S. Inouye, A. Chikkatur, D. Stamper-Kurn, J. Stenger, D. Pritchard, and W. Ketterle, Science **285**, 571 (1999).
[21] T. Bienaimé, S. Bux, E. Lucioni, Ph. W. Courteille, N. Piovella, and R. Kaiser, Physical Review Letters **104**, 183602 (2010).
[22] S. Das, G. S. Agarwal, and M. O. Scully, Physical Review Letters **101**, 153601 (2008).
[23] N. Piovella, Phys. Rev. A **106**, 023701 (2022).
[24] R. A. de Oliveira, M. S. Mendes, W. S. Martins, P. L. Saldanha, J. W. R. Tabosa, and D. Felinto, Physical Review A **90**, 023848 (2014).
[25] S. D. Jenkins, J. Ruostekoski, J. Javanainen, R. Bourgain, S. Jennewein, Y. R. P. Sortais, and A. Browaeys, Physical Review Letters **116**, 183601 (2016).
[26] L. Pucci, A. Roy, T. S. do Espírito Santo, R. Kaiser, M. Kastner, and R. Bachelard, Physical Review A **95**, 053625 (2017).
[27] J. Chabé, M.-T. Rouabah, L. Bellando, T. Bienaimé, N. Piovella, R. Bachelard, and R. Kaiser, Phys. Rev. A **89**, 043833 (2014).
[28] P. Weiss, M. O. Araújo, R. Kaiser, and W. Guerin, New Journal of Physics 20, 063024 (2018).
[29] S. L. Bromley, B. Zhu, M. Bishof, X. Zhang, T. Bothwell, J. Schachenmayer, T. L. Nicholson, R. Kaiser, S. F. Yelin, M. D. Lukin, et al., Nature Communications **7**, 11039 (2016).
[30] P. Weiss, A. Cipris, M. O. Araújo, R. Kaiser, and W. Guerin, Phys. Rev. A **100**, 033833 (2019).
[31] J. G. Bohnet, Z. Chen, J. M. Weiner, D. Meiser, M. J. Holland, and J. K. Thompson, Nature **484**, 78 (2012).
[32] L.-M. Duan, M. D. Lukin, J. I. Cirac, and P. Zoller, Nature **414**, 413 (2001).
[33] H. B. G. Casimir and D. Polder, Phys. Rev. **73**, 360 (1948).
[34] M. Fichet, F. Schuller, D. Bloch, and M. Ducloy, Phys. Rev. A **51**, 1553 (1995).
[35] M.-P. Gorza and M. Ducloy, The European Physical Journal D-Atomic, Molecular, Optical and Plasma Physics **40**, 343 (2006).
[36] J. M. Wylie and J. E. Sipe, Phys. Rev. A **30**, 1185 (1984).
[37] H. Failache, S. Saltiel, M. Fichet, D. Bloch, and M. Ducloy, Phys. Rev. Lett. **83**, 5467 (1999).
[38] H. Failache, S. Saltiel, A. Fischer, D. Bloch, and M. Ducloy, Phys. Rev. Lett. **88**, 243603 (2002).
[39] G. Barton, Proceedings of the Royal Society of London. Series A: Mathematical, Physical and Engineering Sciences **453**, 2461 (1997).
[40] A. Laliotis and M. Ducloy, Phys. Rev. A **91**, 052506 (2015).
[41] A. Laliotis, T. P. de Silans, I. Maurin, M. Ducloy, and D. Bloch, Nature communications **5**, 4364 (2014).
[42] J. C. de Aquino Carvalho, I. Maurin, P. Chaves de Souza Segundo, A. Laliotis, D. de Sousa Meneses, and D. Bloch, Phys. Rev. Lett. **131**, 143801 (2023).
[43] M. S. Tomăs, Phys. Rev. A **51**, 2545 (1995).
[44] H. T. Dung, L. Knöll, and D.-G. Welsch, Phys. Rev. A **65**, 043813 (2002).
[45] T. J. Arruda, R. Bachelard, J. Weiner, S. Slama, and Ph. W. Courteille, Phys. Rev. A **101**, 023828 (2020).
[46] S. Fuchs and S. Y. Buhmann, Europhys. Lett. **124**, 34003 (2018).
[47] K. Sinha, B. P. Venkatesh, and P. Meystre, Phys. Rev. Lett. **121**, 183605 (2018).
[48] R. Jones, J. A. Needham, I. Lesanovsky, F. Intravaia, and B. Olmos, Phys. Rev. A **97**, 053841 (2018).
[49] M. O. Scully, Phys. Rev. Lett. **115**, 243602 (2015).
[50] A. C. Santos, A. Cidrim, C. J. Villas-Boas, R. Kaiser, and R. Bachelard, Phys. Rev. A **105**, 053715 (2022).
[51] S. Y. Buhmann, Dispersion forces I & II , Springer Tracts in Modern Physics **248**, 287 (Springer-Verlag Berlin Heidelberg, 2012).
[52] R. H. Lehmberg, Physical Review A **2**, 883 (1970).
[53] T. Bienaimé, R. Bachelard, N. Piovella, and R. Kaiser, Fortschritte der Physik **61**, 377 (2013).
[54] A. Cipris, R. Bachelard, R. Kaiser, and W. Guerin, Phys. Rev. A **103**, 033714 (2021).
[55] M. O. Araújo, W. Guerin, and R. Kaiser, Journal of Modern Optics **65**, 1345 (2018).
[56] O. S. Heavens, J. Opt. Soc. Am. **51**, 1058 (1961).
[57] M. S. Safronova, U. I. Safronova, and C. W. Clark, Phys. Rev. A **94**, 012505 (2016).
[58] T. J. Arruda, R. Bachelard, J. Weiner, S. Slama, and Ph. W. Courteille, Phys. Rev. A **96**, 043869 (2017).
[59] B. Olmos, D. Yu, Y. Singh, F. Schreck, K. Bongs, and I. Lesanovsky, Phys. Rev. Lett. **110**, 143602 (2013).
[60] W. Guerin and R. Kaiser, Physical Review A **95**, 053865 (2017).
[61] A. Piñeiro Orioli and A. M. Rey, Phys. Rev. A **101**, 043816 (2020).
[62] We have considered same dipole orientations for simplicity, in order to simplify Eqs. (5) and (9). For a full treatment, see, e.g., ref. [44].